$R\left(D^{(*)}\right)$ measurement using the hadronic tag algorithm at the Belle II experiment

Kazuki Kojima[*1], Qi-Dong Zhou[†2,3], Toru Iijima[‡1,2,4], Koji Hara[§4],
Kodai Matsuoka[¶2,4], Katsuro Nakamura[∥4], Taichiro Koga[**4],
for the Belle II Collaboration

[1]Graduate School of Science, Nagoya University, Nagoya, Japan
[2]Kobayashi-Maskawa Institute (KMI), Nagoya University, Nagoya, Japan
[3]Institute of Advanced Research (IAR), Nagoya University, Nagoya, Japan
[4]High Energy Accelerator Research Organization (KEK), Tsukuba, Japan

September 17, 2022

Version 1

Abstract

The global average of $R\left(D^{(*)}\right)$ measurements deviates from the Standard Model by 3.3σ [1], which indicates a violation of lepton universality. Here, we present some preliminary results based on simulation for a first measurement of $R\left(D^{*}\right)$ with the hadronic tag algorithm at the Belle II experiment using 189.3fb^{-1}. In particular, this note summarizes plots and evaluated results of the expected statistical sensitivity and a part of systematic uncertainties that was presented at the 2022 Autumn Meeting of the Physical Society of Japan held from September 6th to 8th, 2022. The details of the analysis are described in `BELLE2-NOTE-PH-2022-032` [2].

---

[*]kojima@hepl.phys.nagoya-u.ac.jp

[†]qzhou@hepl.phys.nagoya-u.ac.jp

[‡]iijima@hepl.phys.nagoya-u.ac.jp

[§]koji.hara@kek.jp

[¶]matsuoka@post.kek.jp

[∥]katsuro@post.kek.jp

[**]taichiro@post.kek.jp

List of Figures

List of Tables

Table 1: Definition of ΔM_{D^*} side band regions, where $\Delta M_{D^*} \equiv M_{D^*} - M_D$.

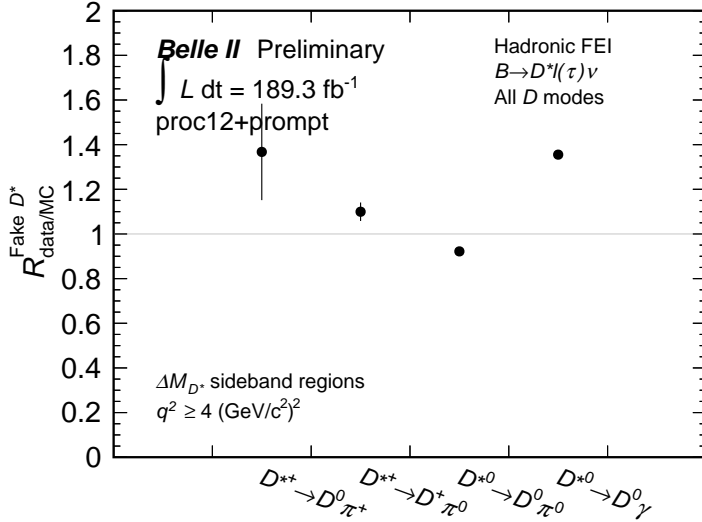| D^* decay	ΔM_{D^*} side band region [GeV/c^2]
$D^{*+} \to D^0\pi^+$	$0.140 < \Delta M_{D^*} < 0.141, 0.155 < \Delta M_{D^*} < 0.170$
$D^{*+} \to D^+\pi^0$	$0.135 < \Delta M_{D^*} < 0.137, 0.150 < \Delta M_{D^*} < 0.170$
$D^{*0} \to D^0\pi^0$	$0.140 < \Delta M_{D^*} < 0.141, 0.155 < \Delta M_{D^*} < 0.170$
$D^{*0} \to D^0\gamma$	$0.100 < \Delta M_{D^*} < 0.120, 0.170 < \Delta M_{D^*} < 0.190$

Figure 1: MC calibration factors $R_{\text{data/MC}}^{\text{Fake } D^*}$ for the reconstructed $D^*\ell(\tau)\nu$ candidates with a wrongly reconstructed D^* candidate (fake D^* events) for each reconstructed D^* decay modes. The yield calibration of the fake D^* events in the MC is made to control the yield of the largest background among the reconstructed candidates. Both in the data and the MC, the fake D^* yields are determined by the fit on ΔM_{D^*} distributions in ΔM_{D^*} side band regions defined in Table 1. The distributions are fitted with a threshold function (`RooDstD0BG`) for $D^{*+} \to D^0\pi^+$, $D^{*+} \to D^+\pi^0$, and $D^{*0} \to D^0\pi^0$ modes and with a first Chebychev function for $D^{*0} \to D^0\gamma$ mode. The calibration factors are calculated by yield ratios of data and MC obtained from the ΔM_{D^*} side band fits. The uncertainties on the calibration factors are propagated in to the R(D*) fit by including external Gaussian constraints on the yields of fake D^* events.
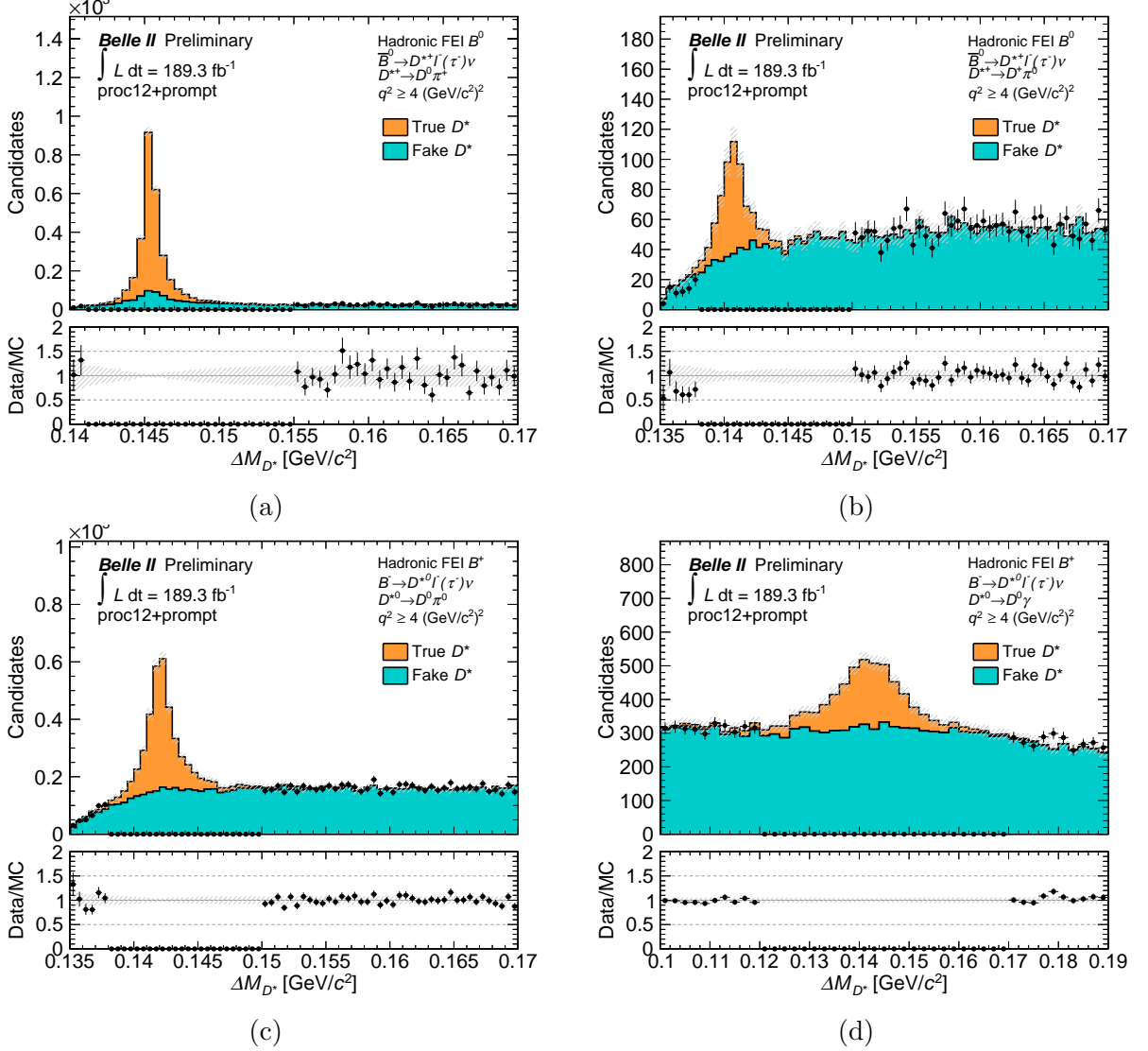
Figure 2: ΔM_{D^*} distributions after the yield calibration on the fake D^* candidates. The distributions of $D^{*+} \to D^0\pi^+$, $D^{*+} \to D^+\pi^0$, $D^{*0} \to D^0\pi^0$, and $D^{*0} \to D^0\gamma$ modes are shown in Figures (a), (b), (c), and (d), respectively. The black points are data. The histograms of reconstructed candidates with a correctly reconstructed D^* candidate (orange) and with a wrongly reconstructed D^* candidate with the calibration (light blue) in the MC are stacked. The true and fake D^* candidates are discriminated based on MC truth matching. In cases where the MC truth matching fails, D^* candidates are categorized as the fake D^* candidates. In Figure (a), a slight peak is observed on the fake D^* distribution due to MC matching failing. The distributions show good agreements between the data and the MC in the ΔM_{D^*} side band regions.
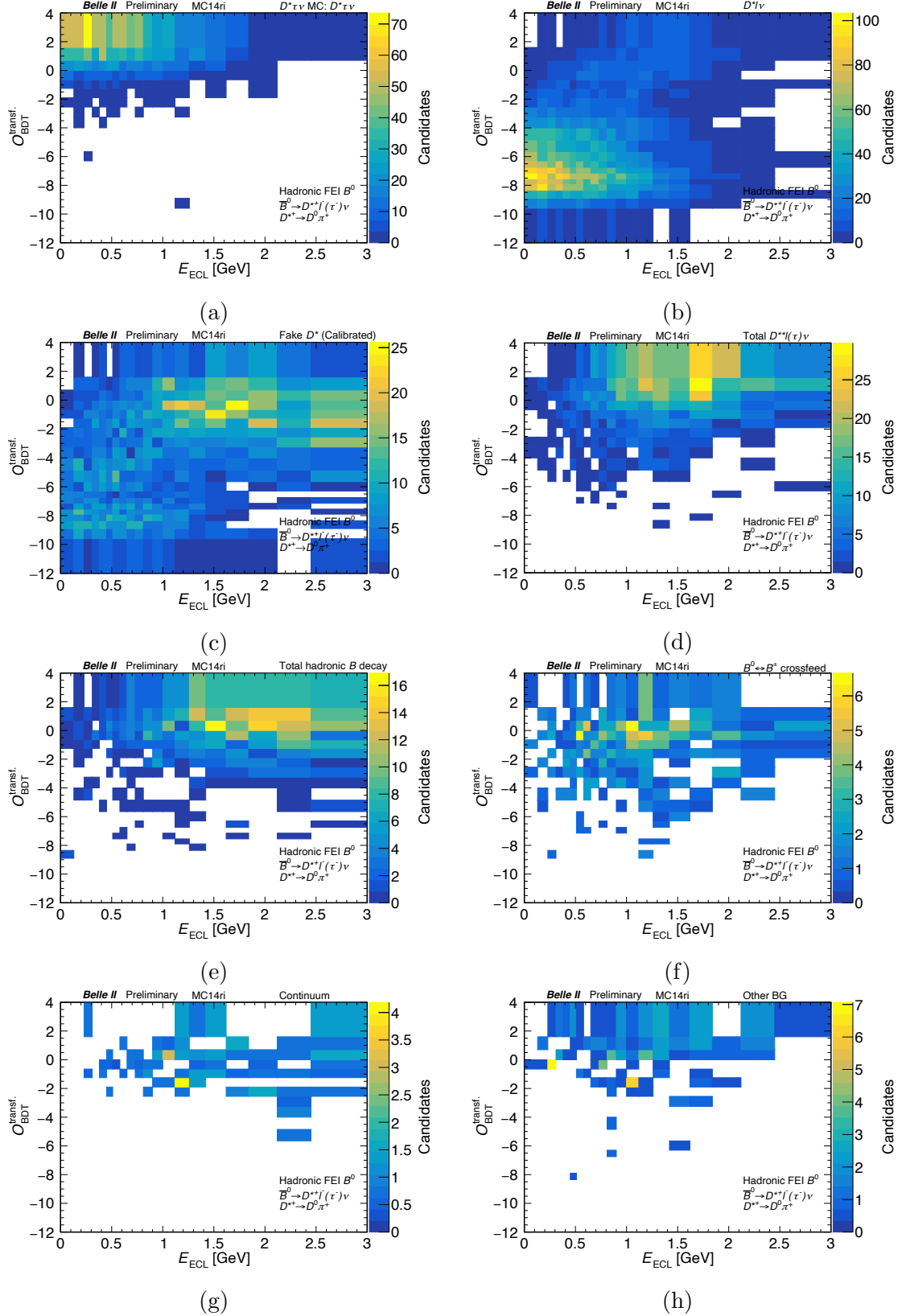
Figure 3: Two-dimensional histogram PDFs of E_{ECL} and $\mathcal{O}_{\mathrm{BDT}}^{\mathrm{transf.}}$ for the $D^{*+} \to D^0 \pi^+$ mode, where E_{ECL} is extra energy of the electromagnetic calorimeter not used for the reconstruction and $\mathcal{O}_{\mathrm{BDT}}^{\mathrm{transf.}}$ is transformed output variable of FastBDT for the enhancement of the $\bar{B} \to D^* \tau^- \bar{\nu}_\tau$ events. The histogram correspond to the following signal and background contributions; (a) $\bar{B} \to D^* \tau^- \bar{\nu}_\tau$, (b) $\bar{B} \to D^* \ell^- \bar{\nu}_\ell$, (c) background events with a fake D^* candidate, (d) $\bar{B} \to D^{**} \ell^- \bar{\nu}_\ell$, (e) hadronic B decays, (f) $B^0 \leftrightarrow B^+$ cross feed of semi-leptonic B decays, (g) $q\bar{q}$ events ($q = u, d, s, c$), and (h) other background events. (d) – (h) are background events with a true D^* candidate.
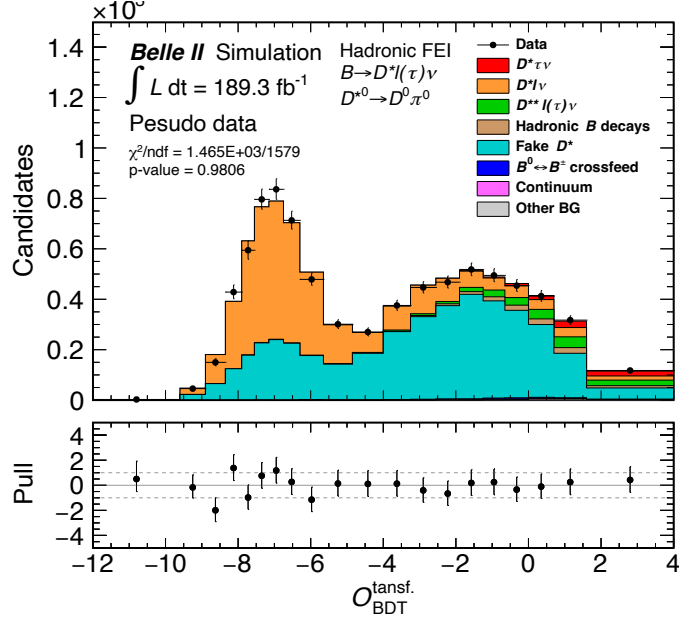
Figure 4: Fitted distributions projected on $\mathcal{O}_{\mathrm{BDT}}^{\mathrm{transf.}}$ in a single pseudo data set corresponding to 189.3 fb^{-1}. The pseudo data are created under an assumption of the SM expectation of $R\,(D^*) = 0.254$. The value of $R\,(D^*)$ is extracted by a simultaneous fit on four two-dimensional distributions of the four D^* decay modes, $D^{*+} \rightarrow D^0\pi^+$, $D^{*+} \rightarrow D^+\pi^0$, $D^{*0} \rightarrow D^0\pi^0$, and $D^{*0} \rightarrow D^0\gamma$. Here, the fitted distribution for the $D^{*0} \rightarrow D^0\pi^0$ mode is shown among the four D^* decay modes in the simultaneous fit. The red and orange histograms show the fit contribution of correctly reconstructed candidates of the signal mode $\bar{B} \rightarrow D^*\tau^-\bar{\nu}_\tau$ and correctly reconstructed candidates of the normalization mode $\bar{B} \rightarrow D^*\ell^-\bar{\nu}_\ell$, respectively.
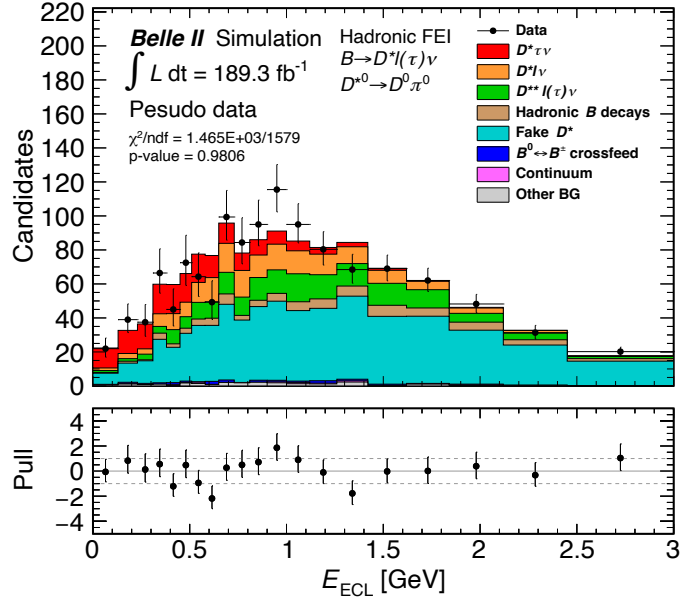
Figure 5: Fitted distributions projected on E_{ECL} with a signal-enhanced selection of $\mathcal{O}_{\text{BDT}}^{\text{transf.}} > 0.0$ in the same single pseudo data set as in Figure 4. In the region of $\mathcal{O}_{\text{BDT}}^{\text{transf.}} > 0.0$, more than 85% of the correctly reconstructed $\bar{B} \to D^* \tau^- \bar{\nu}_\tau$ events are retained while over 85% of the $\bar{B} \to D^* \ell^- \bar{\nu}_\ell$ events and background events are excluded. Here, the fitted distribution for the $D^{*0} \to D^0 \pi^0$ mode is shown among the four D^* decay modes in the simultaneous fit.
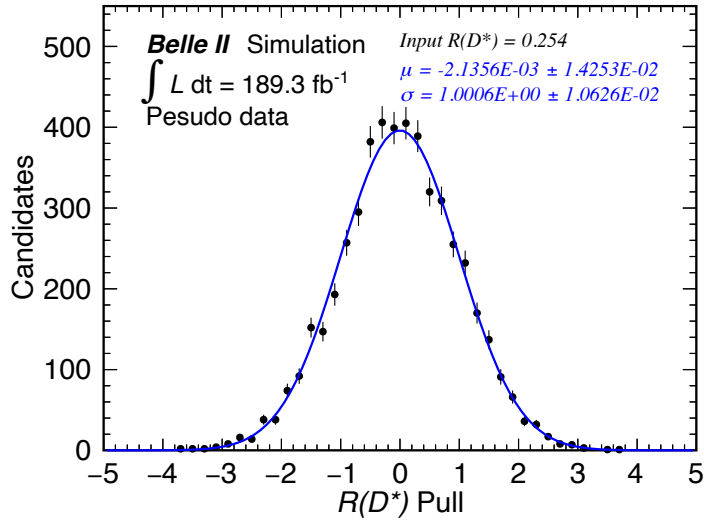
Figure 6: Pull distribution of $R\left(D^*\right)$ values extracted in fits to 5,000 pseudo data samples with a luminosity corresponding to 189.3 fb^{-1}. The pseudo data are created under an assumption of the SM expectation of $R\left(D^*\right) = 0.254$. The mean μ and standard deviation σ are obtained by a fit of a single Gaussian function on the pull distribution shown by the blue line. The fit values are $\mu = -0.002 \pm 0.014$ and $\sigma = 1.001 \pm 0.011$. They are consistent with zero and one, respectively.

8

Table 2: Evaluated results of expected uncertainties at the SM expectation of $R(D^*) = 0.254$ with 189.3 fb^{-1} data at the Belle II experiment for major sources of systematic uncertainty from the previous Belle measurement [3]. The right-most column shows systematic uncertainties in the Belle experiment. So far, for the Belle II measurement, we have evaluated the uncertainty from $\bar{B} \to D^*\tau^-\bar{\nu}_\tau$ composition and hadronic B decay composition. Uncertainties from reconstruction efficiencies, form factors, and PDF shapes still are under evaluation. The uncertainty of $\bar{B} \to D^{**}\ell^-\bar{\nu}_\ell$ is caused by uncertainties on branching ratios of $\bar{B} \to D^{**}\ell^-\bar{\nu}_\ell$ decays and decay modeling of non-resonant $\bar{B} \to D^{(*)}\pi(\pi)\ell^-\bar{\nu}_\ell$ decays. The uncertainty of hadronic B decays is induced by uncertainties on their branching ratios. We evaluate the uncertainties with 1,000 sets of variation of the PDF shapes according to uncertainties on the branching ratios or with replacement of the PDF shapes with those of resonant $\bar{B} \to D^{**}\ell^-\bar{\nu}_\ell$ decays. The uncertainty of reconstruction efficiency comes from the uncertainties of evaluated results of the detector performance, such as the particle identification efficiencies and the tracking efficiencies. The form factors on $\bar{B} \to D\ell^-\bar{\nu}_\ell$, $\bar{B} \to D^*\ell^-\bar{\nu}_\ell$, and $\bar{B} \to D^{**}\ell^-\bar{\nu}_\ell$ could vary the PDF shapes according to their uncertainties and the bias on the $R(D^*)$ fit is evaluated as their systematic uncertainty. We take into account the MC statistics for the PDF creation and disagreements between data and MC as the uncertainty on the PDF shapes.

Source	Systematic uncertainty	
	Belle II	Belle
$\bar{B} \to D^*\tau^-\bar{\nu}_\tau$ composition	$^{+4.6\%}_{-3.9\%}$	3.0%
Reconstruction efficiency		B^0: 2.5%, B^+: 1.2%
Form factor	Under evaluation	1.5%
PDF shape		1.3%
Hadronic B decay composition	$^{+0.7\%}_{-0.3\%}$	—
Total		5.2%

9 References

[1] Y. Amhis et al. Averages of b-hadron, c-hadron, and τ-lepton properties as of 2021. 6 2022.

[2] K. Kazuki et al. Measurement of $R(D^*)$ with the hadronic FEI tagging method using ICHEP 2022 dataset. 2022.

[3] M. Huschle et al. Measurement of the branching ratio of $\bar{B} \to D^{(*)}\tau^-\bar{\nu}_\tau$ relative to $\bar{B} \to D^{(*)}\ell^-\bar{\nu}_\ell$ decays with hadronic tagging at Belle. *Phys. Rev. D*, 92(7):072014, 2015.